

1 **Microbiome Determinants and Physiological Effects of the Benzoate-Hippurate**  
2 **Microbial-Host Co-Metabolic Pathway**

3  
4 François Brial<sup>1,17</sup>, Julien Chilloux<sup>2,17</sup>, Trine Nielsen<sup>3,17</sup>, Sara Vieira-Silva<sup>4,5,17</sup>, Gwen Falony<sup>4,5</sup>,  
5 Lesley Hoyles<sup>2,6</sup>, Ana L. Neves<sup>2</sup>, Andrea Rodriguez-Martinez<sup>2</sup>, Ghiwa Ishac Mouawad<sup>1</sup>,  
6 Nicolas Pons<sup>7</sup>, Sofia Forslund<sup>8,9</sup>, Emmanuelle Le Chatelier<sup>7</sup>, Aurélie M. Le Lay<sup>1</sup>, Jeremy K  
7 Nicholson<sup>2</sup>, Torben Hansen<sup>3</sup>, MetaHIT consortium, Karine Clément<sup>11,12</sup>, Peer Bork<sup>7,13</sup>, S.  
8 Dusko Ehrlich<sup>14,15</sup>, Jeroen Raes<sup>4,5,18</sup>, Oluf Pedersen<sup>3,18</sup>, Dominique Gauguier<sup>1,2,16,18</sup>, Marc-  
9 Emmanuel Dumas<sup>2,16,18</sup>

10  
11 <sup>1</sup> Université de Paris, INSERM UMRS 1124, 45 rue des Saints Pères, 75006 Paris, France.  
12 <sup>2</sup> Imperial College London, Division of Computational and Systems Medicine, Dept of Surgery  
13 and Cancer, Faculty of Medicine, Sir Alexander Fleming building, Exhibition Road, South  
14 Kensington, London SW7 2AZ, UK.  
15 <sup>3</sup> The Novo Nordisk Foundation Center for Basic Metabolic Research, Faculty of Health and  
16 Medical Sciences, University of Copenhagen, DK-2200 Copenhagen, Denmark.  
17 <sup>4</sup> Laboratory of Molecular Bacteriology, Department of Microbiology and Immunology, Rega  
18 Institute, KU Leuven, Herestraat 49, B-3000 Leuven, Belgium.  
19 <sup>5</sup> Center for Microbiology, VIB, Kasteelpark Arenberg 31, B-3000 Leuven, Belgium.  
20 <sup>6</sup> Nottingham Trent University, Department of Biosciences, School of Science and  
21 Technology, Clifton, Nottingham NG11 8NS, UK.  
22 <sup>6</sup> Nottingham Trent University, Department of Biosciences, School of Science and  
23 Technology, Clifton, Nottingham NG11 8NS, UK.  
24 <sup>7</sup> MGP MetaGénoPolis, INRA, Université Paris-Saclay, 78350 Jouy en Josas, France.  
25 <sup>8</sup> Structural and Computational Biology Unit, European Molecular Biology Laboratory, 69117  
26 Heidelberg, Germany.  
27 <sup>9</sup> Max Delbrück Centre for Molecular Medicine, Berlin, Germany.  
28 <sup>10</sup> Experimental and Clinical Research Center, a joint operation of the Max Delbrück Center  
29 in the Helmholtz Association and the Charité University Hospital, Berlin, Germany  
30 <sup>11</sup> INSERM, U1166, team 6 Nutriomique, Université Pierre et Marie Curie-Paris 6, Paris,  
31 France.  
32 <sup>12</sup> Institute of Cardiometabolism and Nutrition (ICAN), Assistance Publique-Hôpitaux de  
33 Paris, Pitié-Salpêtrière Hospital, Nutrition Department, Paris, France.  
34 <sup>13</sup> Department of Bioinformatic Biocentrum, Würzburg University, 97074 Würzburg, Germany  
35 <sup>14</sup> Institut National de la Recherche Agronomique, 78350 Jouy en Josas, France.

36 <sup>15</sup>Centre for Host-Microbiome Interactions, Dental Institute Central Office, King's College  
37 London, Guy's Hospital, London, UK.

38 <sup>16</sup>McGill University and Genome Quebec Innovation Centre, 740 Doctor Penfield Avenue,  
39 Montréal, QC, H3A 0G1, Canada.

40 <sup>17</sup>Co-first authors.

41 <sup>18</sup>Senior authors.

42 Correspondence should be addressed to M.-E.D. [m.dumas@imperial.ac.uk](mailto:m.dumas@imperial.ac.uk) or

43 D.G.[dominique.gauguier@inserm.fr](mailto:dominique.gauguier@inserm.fr)

44

45 **ABSTRACT**

46

47 **Objective.** Gut microbial products are involved in type 2 diabetes, obesity and insulin  
48 resistance. In particular, hippurate, a hepatic phase 2 conjugation product of microbial  
49 benzoate metabolism, has been associated with a healthy phenotype. This study aims to  
50 identify metagenomic determinants and test protective effects of hippurate.

51

52 **Design.** We profiled the urine metabolome by  $^1\text{H}$  Nuclear Magnetic Resonance (NMR)  
53 spectroscopy to derive associations with metagenomic sequences in 271 middle-aged  
54 Danish individuals to identify dietary patterns in which urine hippurate levels were associated  
55 with health benefits. We follow up with benzoate and hippurate infusion in mice to  
56 demonstrate causality on clinical phenotypes.

57

58 **Results.** In-depth analysis identifies that the urine hippurate concentration is associated with  
59 microbial gene richness, microbial functional redundancy as well as functional modules for  
60 microbial benzoate biosynthetic pathways across several enterotypes. Through dietary  
61 stratification, we identify a subset of study participants consuming a diet rich in saturated fat  
62 in which urine hippurate, independently of gene richness, accounts for links with metabolic  
63 health that we previously associated with gene richness. We then demonstrate causality *in*  
64 *vivo* through chronic subcutaneous infusions of hippurate or benzoate (20 nmol/day)  
65 resulting in improved glycemic control in mice fed a high-fat diet. Hippurate improved insulin  
66 secretion through increased  $\beta$ -cell mass and reduced liver inflammation and fibrosis,  
67 whereas benzoate treatment resulted in liver inflammation.

68

69 **Conclusion.** Our translational study shows that the benzoate-hippurate pathway brings a  
70 range of metabolic improvements in the context of high-fat diets, highlighting the potential of  
71 hippurate as a mediator of metabolic health.

72

73

74

75 **INTRODUCTION**

76

77 The human obesity epidemic raises the risk of type 2 diabetes and cardiovascular disease.  
78 Dysbiosis of the gut microbiome is now recognised as a key feature of these disorders.[1]  
79 The microbiome collectively encodes up to 10 million different microbial genes.[2,3] In  
80 particular, gene richness has been proposed as a marker of ecological diversity mirroring  
81 improvements in metabolic health.[4,5] Although the microbiome directly impacts various  
82 biological processes of the host through production or degradation of a multitude of  
83 compounds, the vast majority of molecules involved in this chemical crosstalk remains  
84 elusive.[6-9]

85 There is growing evidence that hippurate, one of the most abundant microbial-host co-  
86 metabolites in human urine, is positively associated with metabolic health through inverse  
87 associations with blood pressure, fatty liver disease, visceral fat mass and Crohn's  
88 disease.[10-14] Its microbial precursor, benzoate is taken up by organic anion transporter  
89 MCT2[15] and conjugated with glycine in the liver and kidney to form hippurate. We showed  
90 in a genetic cross between diabetic and normoglycemic rat strains that serum benzoate  
91 under host genome control.[16] Hippurate was recently shown to be associated both with  
92 microbiota diversity based on 16S rRNA gene sequencing[17] and with reduced risk of  
93 metabolic syndrome.[13]

94 However, there is a critical need for an in-depth characterization of the complex nutrition-  
95 microbiome-host interaction in the benzoate-hippurate pathway, in relation to: i) associations  
96 with enterotype, gene richness and functional redundancy, ii) population stratification  
97 according to nutritional patterns to identify patient sub-groups in which hippurate improves  
98 metabolic health, and iii) translational elucidation of these effects on host phenotypes *in vivo*.  
99 To address these specific points, we characterized the urinary metabolome and the fecal  
100 microbiome of 271 middle-aged non-diabetic Danish individuals from the MetaHIT study.[4]  
101 Through dietary stratification we delineate the complex interaction between dietary intake,  
102 microbiome and metabolome its impact on body weight, immune and metabolic markers,  
103 which we further confirm and characterise in a mouse model of diet-induced obesity and  
104 diabetes.

105

106 **METHODS**

107

108 **Human subjects**

109 All analyses were done on non-diabetic Danish individuals from the MetaHIT study  
110 (n=271),[4,18] including the subset of 193 individuals who completed a validated food  
111 frequency questionnaire (FFQ).[19] The study was approved by the Ethical Committees of  
112 the Capital Region of Denmark (HC-2008-017 and H-15000306) and was in accordance with  
113 the principles of the Declaration of Helsinki. All individuals gave written informed consent  
114 before participating in the study. Sampling and clinical phenotyping were performed as  
115 described previously.[4,18] In short, all study participants were recruited from the population-  
116 based Inter99 study.[20]. The study program consisted of two visits with approximately 14  
117 days apart. At the first visit all participants were examined in the morning after an overnight  
118 fast. Blood sampling was performed at the fasting state, and urine was collected upon arrival  
119 at the centre. At the second visit, a Dual Energy X-Ray Absorptiometry (DXA) scan was  
120 performed. Serum glycine levels were previously assessed.[19] Estimated glomerular  
121 filtration rate (eGFR) was calculated with the CKD-EPI formula with age, gender and  
122 creatinine (μmol/L) and without ethnicity factor.[21]

123 **Dietary assessment**

124 A subset of the study participants (n=193) completed a validated FFQ in order to obtain  
125 information on their habitual dietary habits.[22] The FFQ gathered dietary information from  
126 all meals during a day and the intake frequencies within the past months were recorded. The  
127 dietary data were evaluated by determining the consumed quantity and multiplying the  
128 portion size by the corresponding consumption frequency as reported in the FFQ. Standard  
129 portion sizes for women and men, separately, were used in this calculation; all food items in  
130 the FFQ were linked to food items in the Danish Food Composition Databank as previously  
131 described.[19] Estimation of daily intake of macro-and micronutrients for each participant  
132 was based on calculations in the software program FoodCalc version1.3  
133 (<http://www.ibt.ku.dk/jesper/FoodCalc/Default.htm>).

134 **Sample collection**

135 Fecal sample collection and analysys was performed as previously described.[4] Urine was  
136 collected at the first visit upon arrival at the study site and stored at -80°C until analysis.

137 **Metabolic profiling**

138 Urine samples were randomized, prepared and measured on a NMR spectrometer (Bruker)  
139 operating at 600.22 MHz  $^1\text{H}$  frequency using previously published experimental  
140 parameters[23] The  $^1\text{H}$  NMR spectra were then pre-processed and analyzed as previously

141 reported[10] using Statistical Recoupling of Variables-algorithm.[24] Structural assignment  
142 was performed as reviewed in [25], using in-house and publicly available databases.

#### 143 **Metagenomics**

144 Shotgun sequencing of microbial DNA and metagenomics processing workflow for gene  
145 richness was performed as previously published.[4] Sequences were mapped onto the  
146 previously released integrated gene catalog.[2] Following the previously published  
147 strategy,[26] we built a novel set of manually curated gut-specific metabolic modules  
148 (GMMs) to describe and map microbial phenylpropanoid metabolism from shotgun  
149 metagenomic data. The set of 20 modules, following KEGG syntax, is provided in  
150 supplement, including references to the original publications where pathways were  
151 discovered and described (***Supplementary List***).

#### 152 **Univariate statistical analysis**

153 A ROUT test was performed to identify potential outliers (Q=1%). For statistical comparisons  
154 between study groups, normality was tested using D'Agostino-Pearson omnibus normality  
155 test, then one-way ANOVA was used, followed by Tukey's HSD post hoc testing when data  
156 were normally distributed, otherwise groups were compared using the two-tailed Mann-  
157 Whitney test. Data are displayed as mean  $\pm$  s.e.m in all figures. Multiple testing corrections  
158 were performed using Storey's procedure.[27]

#### 159 **Multivariate statistics**

160 Probabilistic principal component analysis (PCA) was performed using MATLAB R2014a  
161 function 'ppca' to handle missing values. Unconstrained ordination was performed using  
162 principal coordinates analysis (PCoA) to visualize inter-individual variation in microbiota  
163 composition using Bray-Curtis dissimilarity on the genus-level abundance matrix using the R  
164 package *vegan*.[28] Distance based Redundancy Analysis (dbRDA) was used to determine  
165 the cumulative contributions of a matrix of explanatory variables on the response data,  
166 hippurate excretion inter-individual variation (Euclidian distance on log-transformed urine  
167 hippurate concentration matrix) in R package *vegan*.[28]. Orthogonal partial least squares  
168 discriminant analysis (O-PLS-DA) was performed in MATLAB R2014a for supervised  
169 multivariate analysis as previously described.[29] The predictive capability of O-PLS-DA  
170 models was evaluated through 7-fold cross-validation[29] to compute  $Q^2_{Y\hat{Y}}$  goodness-of-  
171 prediction parameters. The empirical significance of the  $Q^2_{Y\hat{Y}}$  parameter was evaluated by  
172 random permutation testing (10,000 iterations).[30]

#### 173 **Animal experiments**

174 Six-week-old C57BL/6J male mice (Janvier Labs, Courtaboeuf, France) were maintained in  
175 specific pathogen free condition on a 12h light/dark cycle and fed a standard chow diet

176 (R04-40, Safe, Augy, France) for a week. Groups of 10 randomly selected mice were then  
177 fed either control chow diet (CHD) (D 12450Ki, Research diets, NJ) or high fat (60% fat and  
178 sucrose) diet (HFD) (D12492i, Research diets, NJ). One week later, osmotic minipumps  
179 (Alzet® model 2006, Charles River Lab France, l'Arbresle, France) filled with a solution of  
180 either hippuric acid or benzoic acid (5.55mM in 0.9% NaCl) (Sigma Aldrich, St Quentin,  
181 France) were inserted subcutaneously under isoflurane anesthesia. The metabolites were  
182 delivered at a rate of 0.15  $\mu$ L/hour over a 42-day period (20 nmol/day).

183 Glycemia and body weight were recorded weekly. After 3 weeks of metabolite treatment,  
184 mice underwent an intra-peritoneal glucose tolerance test (IPGTT, 2g/kg). Blood was  
185 collected from the tail vein before glucose injection and 15, 30, 60 and 120 minutes  
186 afterwards to determine glycemia using an Accu-Check® Performa (Roche Diagnostics,  
187 Meylan, France). Cumulative glycemia (AUC) was calculated as the sum of plasma glucose  
188 values during the IPGTT and cumulative glucose increase ( $\Delta G$ ) parameter was calculated  
189 as AUC above the fasting glycemia baseline integrated over the 120 min of the IPGTT.  
190 Insulinemia was determined at baseline and at 30 minutes using insulin ELISA kits  
191 (Mercodia, Uppsala, Sweden). After 6 weeks of metabolite infusion, mice were killed by  
192 decapitation and organs were dissected and weighed. Triglycerides were quantified using a  
193 colorimetric assay (ab65336, Abcam, Paris, France) of liver homogenates. All procedures  
194 were authorized following review by the institutional ethic committee and carried out under  
195 national licence condition (Ref 00486.02).

#### 196 **Histology and immunohistochemistry of animal tissues**

197 Liver fibrogenesis and immunohistochemistry were determined as previously described [31].  
198 An epitope-specific antibody (C27C9) was used for immunohistochemistry detection of  
199 insulin on pancreas sections (8508S Ozyme, Saint Quentin en Yvelines, France).

#### 200 **RNA isolation and quantitative RT-PCR**

201 Liver RNA preparation and reverse transcription were performed as previously reported [31].  
202 Quantitative RT-PCRs were performed using oligonucleotides designed for the genes *Col1*  
203 (Forward: CACCCCAGCGAAGAACTCATA; Reverse:  
204 GCCACCATTGATAGTCTCTCCTAAC) and *Col3* (Forward: GCACAGCAGTCCAACGTAGA;  
205 Reverse: TCTCCAAATGGGATCTCTGG) and using the cyclophilin A housekeeping  
206 gene.[31]

207

208 **RESULTS**

209

210 **Hippurate is the urine metabolite most strongly associated with fecal microbial gene  
211 richness.**

212 To identify microbial and host compounds mediating beneficial effects in metabolic health,  
213 we profiled the urinary metabolome of the MetaHIT population[4] using  $^1\text{H}$  nuclear magnetic  
214 resonance (NMR) spectroscopy to perform a Metabolome-Wide Association Study  
215 (MWAS)[11] for microbial gene richness, a proposed criterion of metabolic and immune  
216 health[4] (Figure 1). We first built an orthogonal partial least squares (O-PLS) regression  
217 model based on the  $^1\text{H}$  NMR spectra to stratify the population by gene richness quartiles  
218 computed using our previously published 10-million integrated gene catalog (IGC)[2] (Figure  
219 1A,  $P=5.8\times 10^{-21}$ ). The cross-validated model significantly predicted variance associated with  
220 gene richness through a permutation test (Figure 1B,  $P=9.7\times 10^{-5}$ , 10,000 randomizations).  
221 Model coefficients for this discrimination revealed hippurate as having the strongest  
222 association with microbial gene count (Figure 1C): individuals with low microbial richness  
223 present significantly lower urinary hippurate levels than individuals with high microbial  
224 richness (Figure 1D,  $P=1.99\times 10^{-9}$ ,  $r^2=0.173$ ). These data support reports of association  
225 between hippurate levels and microbial functional redundancy[26] and Shannon's diversity  
226 index[17] (Figure 1E,  $P=0.024$  and Supplementary Figure 1A,  $P=0.0058$ ).

227

228 Consistent with associations previously reported for microbial gene richness in the MetaHIT  
229 population[4] and associations between hippurate and reduced cardiometabolic disease  
230 risk[11,12,14,17], urinary hippurate significantly correlated with low values for body mass  
231 index (BMI), bodyweight, the homeostasis model assessment of insulin resistance (HOMA-  
232 IR) and fasting circulating levels of IL6, insulin, and C-peptide, whilst adjusting for age and  
233 gender (partial Spearman's rank-based correlations,  $q<0.1$ , Supplementary Figure 1B).  
234 Moreover, stratification on urinary hippurate concentrations in lean ( $\text{BMI} < 25 \text{ kg/m}^2$ ), and  
235 overweight or obese ( $\text{BMI} > 25 \text{ kg/m}^2$ ) individuals showed improved glucose homeostasis in  
236 participants excreting higher levels of hippurate (Supplementary Figure 1C, *median*  
237 *threshold*). These observations depict hippurate, one of the main microbial-mammalian co-  
238 metabolites found in human urine, as a key molecular marker associated with gene richness  
239 which may underlie some of its health benefits. These results however raise questions  
240 related to the entanglement of gene richness and hippurate as potential markers of  
241 health[13,17]. Adjusting for hippurate weakens associations between gene richness and  
242 bioclinical variables (Supplementary Figure 1B), consistent with the idea that hippurate could

243 mediate some of the observed benefits for subjects with higher gene richness. However,  
244 hippurate associations with bioclinical variables adjusted for gene richness are no longer  
245 significant, suggesting that the gene richness signal overrides hippurate associations in the  
246 presence of confounding variation affecting urinary concentrations, such as diet, microbial  
247 synthesis, host conjugation and clearance. Hippurate did not correlate either to glycine  
248 bioavailability, which is required for hippurate synthesis through conjugation with gut  
249 microbial benzoate[32] or kidney function (eGFR) which could limit hippurate synthesis and  
250 clearance (Supplementary Figure 1D-E).

251

## 252 **Microbiome determinants of hippurate production in the phenylpropanoid pathway**

253 To characterize the microbial determinants of benzoate production, we next focussed on  
254 high-throughput shotgun sequencing fecal metagenomics data (n=271). We functionally  
255 annotated functions of the IGC to KEGG Orthology (KO) groups and found 2,733 KEGG and  
256 6,931 EggNOG modules positively associated with urine hippurate levels (pFDR<0.05,  
257 Supplementary Tables S1-2). Of specifically curated enzymatic modules[26] involved in  
258 microbial benzoate metabolism (4 aerobic and 15 anaerobic; Supplementary List), only three  
259 modules significantly correlated with urine hippurate levels: MC0004 (detected in 271  
260 samples) corresponding to a 2-enoate reductase converting cinnamic acid into 3-(3-  
261 hydroxyphenyl)-propionic acid, MC0005 (observed in 201 samples) converting cinnamate  
262 into benzoate and MC0014, a benzoate 4-monooxygenase only observed in fewer than 15%  
263 of individuals (Figure 2A, Supplementary Table S3). Abundance of these modules also  
264 correlated with gene richness (Supplementary Table S4), thereby providing a functional  
265 basis for the association between gene richness and urine hippurate levels observed in this  
266 population (Figure 1). Genes involved in MC0004 and MC0005 were predominantly found in  
267 genomes from unclassified Firmicutes and Clostridiales (Figure 2B, Supplementary Tables  
268 S5-6). Among classified Firmicutes, the genera *Lachnoclostridium*, *Eubacterium* and *Blautia*  
269 harbored MC0004. Conversely, MC0005 was encoded by Proteobacteria, i.e. *Klebsiella*,  
270 *Enterobacter*, *Suterella* and *Comamonas* (Figure 2B). We then mapped these modules into  
271 the enteroscope (as observed on the principal coordinates plot derived from normalized  
272 genus abundances using Bray-Curtis distances,[26] Figure 2C), revealing that the  
273 conversion of cinnamic acid into 3-hydroxy-3-phenylpropionic acid is linked to the  
274 *Ruminococcus* enterotype, while capacity to convert cinnamate to benzoate is more  
275 ubiquitously distributed across gut community types. Phenylpropanoid pathway potential is  
276 increased in the *Ruminococcaceae*-enterotype compared to the *Bacteroides*- or *Prevotella*-  
277 enterotypes, the former being confirmed by analyzing gradients of key taxa instead of

278 enterotypes (Supplementary Table S7). The results altogether suggest a wide range of  
279 substrates, taxa and species are involved in benzoate production, consistent with its  
280 association with gene richness.

281

282 **Urine hippurate levels associate with improved metabolic health in patients with diets**  
283 **rich in meat and saturated fats**

284 We next assessed individual nutritional intake through validated FFQs available in 193  
285 MetaHIT individuals.[19] Associations with metabolic health were stratified according to  
286 multivariate dietary patterns (Figure 3). A PCA of 133 dietary intake descriptors summarises  
287 dietary patterns and loadings highlight four archetypal diets within our population: higher  
288 consumption of fruits and vegetables (n=96) vs. high consumption of meat containing  
289 saturated fats (n=97) on the first principal component (PC1) and carbohydrate-rich foods vs.  
290 fish containing unsaturated fats on PC2 (Figure 3A), a trend which was observed at the food  
291 ingredient and nutrient level (Supplementary Figure 2A-B). It is therefore possible to stratify  
292 the population according to the median of dietary PC1 highlighting contrasts between  
293 healthy (higher consumption of fruit and vegetables) and at-risk (higher consumption of  
294 carbohydrates and meat) diets. Although hippurate was not correlated with the first two  
295 dietary principal components, its dynamic range was similar whilst stratifying according to  
296 the first two principal components (Supplementary Figure 2C-E). To summarise the main  
297 factors influencing inter-individual variation in urine hippurate excretion, we calculated the  
298 cumulative contribution of several covariates using a dbRDA ordination approach (Figure  
299 3B). Gene richness accounted for 12% (P=0.002), followed by MC0020 encoding a  
300 hippurate dehydrolase (4%, P=0.002, observed in 271 subjects) catalysing the  
301 retroconversion of hippurate into benzoate, and HOMA-IR (1.5%, P=0.008; n=265). When  
302 taking diet into account (i.e., PC1 fruits and vegetables vs. meat; n=193) in the dbRDA, gene  
303 richness contributes to 15% (P=0.002), diet adding another 4% (P=0.002) and hippurate  
304 retroconversion 3% (P=0.004), suggesting that the pattern of hippurate associations could  
305 be diet-dependent and requiring further analysis. We therefore stratified the data according  
306 to diet (n=193) using a median threshold for the first dietary principal component,  
307 highlighting a healthy diet associated with vegetables and fruit intake (low PC1 values, n=96)  
308 and an at-risk diet rich in saturated fats derived from meat intake (n=97). For this latter  
309 subset of individuals consuming a diet rich in saturated fats on the first dietary principal  
310 component, urine hippurate levels significantly associated with decreased HOMA-IR,  
311 circulating fasting levels of insulin, fasting associated adipocyte factor (FIAF, also known as  
312 Angiopoietin-like 4, a peroxisome proliferator-activated receptor target gene environmentally

313 modulated by the gut microbiota inhibiting lipoprotein lipase in adipose tissue [33]) and TNF-  
314  $\alpha$ , whilst displaying increased plasma levels of fasting adiponectin (Figure 3C-E,  
315 Supplementary Table S8). Urine hippurate was not associated with any health benefits in the  
316 subsets of participants consuming mostly a fruit and vegetable diet, a pescetarian diet or a  
317 carbohydrate-rich diet (Supplementary Table S8).

318

319 To disentangle contributions arising from hippurate and gene richness to bioclinical variables  
320 in subjects consuming a diet rich in fats, we compared unadjusted and adjusted Spearman's  
321 rank-based correlations (Figure 3H). In the population consuming higher amounts of meat  
322 and saturated fats, elevated urine hippurate levels significantly associated with an increase  
323 in fasting plasma adiponectin and a reduction in adiposity, BMI, HOMA-IR and fasting  
324 plasma insulin, which is consistent with gene richness being significantly associated with an  
325 increase in adiponectin and a decrease in HOMA-IR and fasting plasma insulin. However,  
326 the associations between gene richness and bioclinical variables were no longer significant  
327 when adjusting for urine hippurate levels. Conversely, hippurate associations with insulin  
328 and HOMA-IR were still significant after gene richness adjustment. We exemplified this  
329 through a correlation graph taking into account the correlation between hippurate and gene  
330 richness ( $r=0.44$ ): this unadjusted correlation between gene richness and HOMA-IR  
331 collapses when adjusting for gene richness ( $\rho=0.143$ , n.s.) and is in fact contributed for by  
332 a partial correlation between urine hippurate and HOMA-IR (Figure 3I). The latter finding  
333 suggests a possible preventive role for hippurate in metabolic disease driven by diets high in  
334 meat and saturated fats, independently of gene richness.

335

### 336 **Hippurate and benzoate improve glucose tolerance in HFD-fed mice**

337 To further study the impact of benzoate and hippurate on host physiology, we treated mice  
338 with subcutaneous infusion of hippurate (0.14 mg/kg/day) and benzoate (0.1 mg/kg/day) in  
339 CHD and HFD (Figure 4). Under control diet, metabolite treatments had no effect on body  
340 weight, BMI and fasting glycemia (Supplementary Figure 4). Benzoate caused a significant  
341 elevation of the adiposity index and a reduction of the normalised heart weight  
342 (Supplementary Figure 5A). During an IPGTT, both metabolites induced a slight increase in  
343 glycemia (Figure 4A-B) and  $\Delta G$  parameter (Figure 4C), respectively. Also, hippurate induced  
344 a stronger glucose-stimulated insulin secretion than benzoate, compared to the saline-  
345 treated mice (Figure 4D). Whilst HFD-feeding increased body weight and adiposity,  
346 hyperglycemia and glucose intolerance (Figure 4E-H, Supplementary Figs 4D,E and 5),  
347 mice treated with hippurate or benzoate showed a parallel improvement in glucose tolerance

348 compared to saline-treated controls (Figure 4E). This effect was illustrated by the highly  
349 significant reduction of both the cumulative glycemia during the test (Hippurate vs. control -  
350 23.90% P=0.001, benzoate vs. ctrl -31.52%, P=0.001) and the  $\Delta G$  parameter (Hippurate vs.  
351 ctrl -37.22% P=0.001, benzoate vs ctrl -33.35%, P=0.001) (Figure 4F,G). Hippurate and  
352 benzoate treatments also significantly increased glucose-induced insulin secretion (Figure  
353 4H). These data suggest that both metabolites have the capacity to improve glucose  
354 tolerance and stimulate glucose-induced insulin secretion *in vivo* specifically in diet-induced  
355 obesity and diabetes.

356

### 357 **Effects of hippurate and benzoate on the morphology of pancreatic islets**

358 To investigate the possible cause of stimulated insulin secretion by hippurate and benzoate,  
359 we performed out a histological analysis of pancreatic islet structure. We confirmed that  
360 insulin positive area was increased by hippurate (+194%, P=0.04, one-tailed) or benzoate  
361 (+437%, p=0.02, one-tailed) respectively in mice fed control diet (Figure 5); hippurate  
362 treatment Insulin positive area was also increased in HFD-fed mice treated with hippurate  
363 (+168%, P=0.04, one-tailed). These data suggest that increased  $\beta$ -cell mass may explain  
364 enhanced insulin production and secretion induced by hippurate and benzoate treatment.

365

### 366 **Effects of hippurate and benzoate on liver histopathology and function**

367 Liver triglyceride accumulation, fibrosis and inflammation are hallmarks of structural and  
368 biochemical adaptations to HFD feeding. Liver triglycerides were more elevated in HFD fed  
369 mice ( $29.30 \pm 4.15$  mg/g) than in mice fed control diet ( $8.63 \pm 2.19$  mg/g, P=0.002)  
370 (Supplementary Figure 6). Hepatic triglycerides were not significantly affected by hippurate  
371 or benzoate treatment in either diets. Benzoate induced a singifnican decrease in liver  
372 triglycerides compared to hippurate in HFD (-57.35%, P= 0.02) (Supplementary Figure 6).  
373 We next analysed hepatic fibrosis through quantitative analysis of collagen detected by red  
374 picrosirius staining of histological sections (Figure 6A). Hippurate treatment resulted in a  
375 marked reduction of liver collagen in mice fed control diet (-53.2%) or HFD (-55.7%),  
376 whereas benzoate had no effects on collagen levels in these mice (Figure 6B,C). These  
377 results were confirmed by liver expression of the genes encoding collagen 1 (*Col1*) and  
378 collagen 3 (*Col3*) (Figure 6B,C): hippurate treatment induced a significant reduction of the  
379 expression of *Col1* (-79.89%, P=0.02) and *Col3* (-29.37%, P=0.01) under control diet (Figure  
380 6B). but the effect of the metaolites on *Col1* and *Col3* I HFD was marginal (Figure 6C).  
381 Finally, we assessed the effects of hippurate and benzoate on liver inflammation through  $\alpha$ -  
382 SMA (alpha Smooth Muscle Actin) staining[34,35] (Figure 7A), which is increased by HFD-

383 feeding (+273.86%) (Figure 7B,C). Hippurate induced a marked reduction in  $\alpha$ -SMA staining  
384 in mice fed control diet (-82.71%) or HFD (-94.87%) (Figure 7B,C), suggesting reduced  
385 presence of stellar cells and reduced liver inflammation when compared to saline-treated  
386 controls. In contrast, benzoate treatment in chow diet induced a strongly significant increase  
387 in stellar cells when compared to mice treated with saline (+564%,  $P=10^{-7}$ ) or hippurate  
388 (+3,741%,  $P=10^{-7}$ ), thereby indicating liver inflammation in these mice (Figure 7B).  
389 Collectively, these data show that hippurate decreases fibrosis and inflammation regardless  
390 of diet, whereas benzoate reduces triglycerides and collagen accumulation in obese mice  
391 fed HFD whilst stimulating inflammation in lean mice fed control diet.

392

### 393 **DISCUSSION**

394

395 Integrated analysis of metabolome profiling and deep metagenome sequencing data of 271  
396 middle-aged non-diabetic Danish subjects from the MetaHIT study sample [4] identified  
397 urinary hippurate as the metabolite most significantly associated with microbial gene  
398 richness based on the microbial IGC.[2] This observation largely confirms previous reports  
399 associating hippurate with gene richness in steatosis and bariatric surgery contexts[14,36]  
400 as well as with increased gut microbial diversity as assessed by sequencing the 16S rRNA  
401 gene amplicon.[17] Hippurate having previously been inversely correlated with blood  
402 pressure, obesity and steatosis,[11-14] this study highlights diet-dependent relationships  
403 between microbiota-host co-metabolism of benzoate and hippurate and health benefits  
404 associated with gene richness. Our in-depth dissection of the metagenomic determinants of  
405 urinary hippurate highlighted a series of richness-responsive gene modules functionally  
406 related to benzoate synthesis. These modules are shared across several enterotypes and  
407 taxonomic gradients. Population stratification analyses demonstrated that hippurate only  
408 benefits individuals consuming a diet rich in saturated fats. This hypothesis of a diet-  
409 dependent beneficial health effect of benzoate metabolism was confirmed *in vivo* in a  
410 preclinical model of HFD-induced obesity.

411

### 412 **Hippurate brings diet-dependent metabolic improvements in pancreas and liver**

413 Our study shows that chronic hippurate treatment in a model of obesity induced by HFD-  
414 feeding reduces glucose intolerance, stimulates insulin secretion, enhances  $\beta$ -cell mass and  
415 reduces hepatic inflammation and fibrosis. Metabolomic studies have consistently shown  
416 inverse associations variations between hippurate levels and pathophysiological elements of  
417 the metabolic syndrome. Urinary hippurate is reduced in mouse models of insulin

418 resistance[10] and in rat models of spontaneously occurring hypertension (SHR), type 2  
419 diabetes (Goto Kakizaki, GK) and obesity (Zucker) or the WKY rat.[37-39] This is consistent  
420 with our previous reports showing an inverse association among hippurate, insulin  
421 resistance, hypertension, obesity or liver steatosis[10-12,14] and observations that hippurate  
422 exerts protective effects in  $\beta$ -cells.[40] We also showed in HFD-fed isogenic mice that  
423 urinary hippurate measured before a 3-week HFD induction predicts the future development  
424 of obesity, suggesting that functional variations in microbiome predicts disease risk  
425 independently of genetics.[41] Whilst both hippurate and benzoate have similar *in vivo*  
426 effects, including greatly improved glucose tolerance and stimulation of insulin secretion,  
427 only hippurate results in beneficial effects on increased  $\beta$ -cell mass or reduced liver fibrosis.  
428

#### 429 **The phenylpropanoid-benzoate-hippurate pathway in metabolic health**

430 The range of responses observed in the animal model treated with hippurate and benzoate  
431 depict subtle and context-dependent microbiome–host interactions. Benzoate and its co-  
432 metabolite hippurate are the endproducts of several converging microbial biosynthetic  
433 pathways.[15] The phenylpropanoid pathway is a broad network of reactions connecting a  
434 wide range of dietary substrates such as phenylalanine, quinic acid, shikimic acid or  
435 chlorogenic acid for instance to 4-coumaryl-coA. These pathways lead to much simpler  
436 molecules, benzoate being their common endpoint. Dietary and microbial intermediates  
437 (including cinnamic acids, coumarins, stilbenoids, flavonoids and isoflavonoids) in the  
438 phenylpropanoid and connected pathways are associated with beneficial health  
439 outcomes.[15,42]

440

441 **Conclusion.** Our study depicts hippurate as a pivotal microbial-host co-metabolite mediating  
442 part of the beneficial metabolic improvements associated with high microbial gene richness  
443 in the context of Western-style diets. This work unifies previous reports in which hippurate  
444 was associated improvements in insulin resistance, steatosis, hypertension and obesity[10-  
445 12,14] and microbial ecological diversity.[14,17] Beyond the diversity of microbial  
446 ecosystems and functions associated with hippurate, we uncover beneficial bioactivities in  
447 the liver and pancreas resulting in health benefits in terms of metabolic control, liver  
448 inflammation and fibrosis. Our observations support the existence of diet-dependent  
449 microbial-host metabolic axis in which hippurate partly offsets unhealthy diets, further  
450 exemplifying that the microbiome determines key components of human biochemical  
451 individuality[43] and provides critical diagnostic and therapeutic potential in personalized  
452 nutrition and stratified medicine.[44,45]

453 **Acknowledgements**

454 This research was funded by FP7 METACARDIS HEALTH-F4-2012-305312 with additional  
455 funding from the Metagenopolis grant ANR-11-DPBS-0001 and support of the NIHR Imperial  
456 Biomedical Research Centre. The Novo Nordisk Foundation Center for Basic Metabolic  
457 Research is an independent research institution at the University of Copenhagen partially  
458 funded by an unrestricted donation from the Novo Nordisk Foundation. S.V.S. is funded by  
459 Marie Curie Actions FP7 People COFUND Proposal 267139 (acronym OMICS@VIB) and  
460 the Fund for Scientific Research-Flanders (FWO-V). L.H. was an MRC Intermediate  
461 Research Fellow (MR/L01632X/1).

462

463 **Contributions**

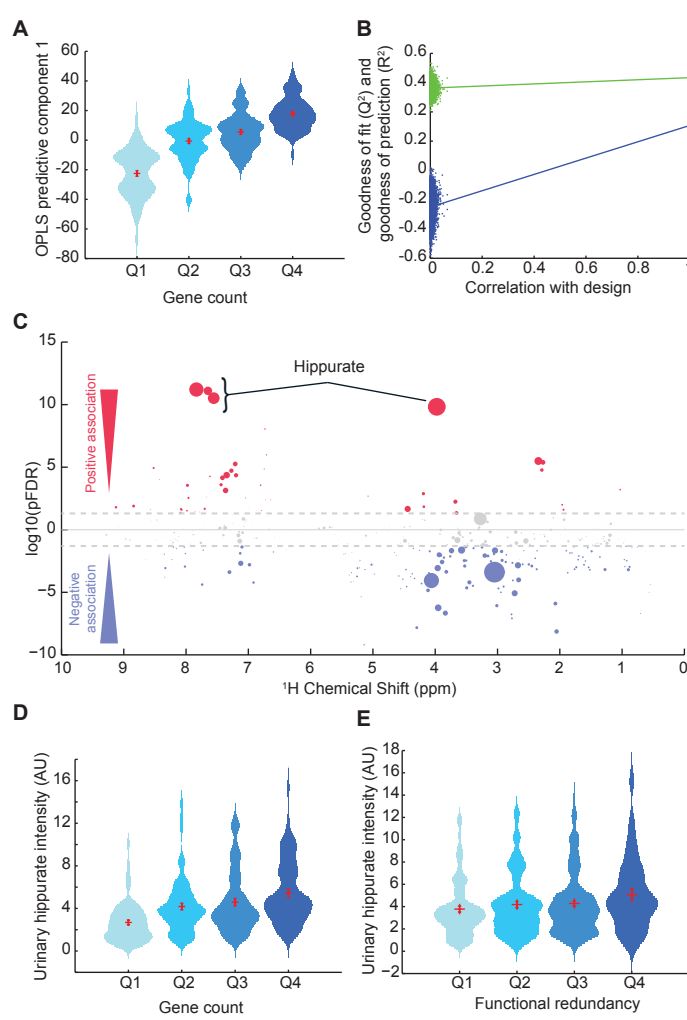
464 F.B. J.C., T.N. and S.V.S. and contributed equally to this work. F.B. J.C. and G.I.M. acquired  
465 data, J.C., T.N., S.V.S. performed analyses, G.F. and S.V.S. curated the gut-specific  
466 metabolic modules, L.H., A.L.N., A.R.M., N.P., S.F., E.L.C., and A.M.L.L. participated in data  
467 collection and processing, J.C., T.N., S.V.S., F.B. and G.F. performed statistical analyses.  
468 M.-E.D., D.G., J.R. and O.P. designed the study. T.H., J.K.N. K.C., P.B., S.D.E., participated  
469 in the study design and interpretation of the results, M.E.D. wrote the manuscript with  
470 contributions from F.B., J.C., T.N., S.V.S, G.F., J.R., O.P and D.G.

471

472 **Competing interests**

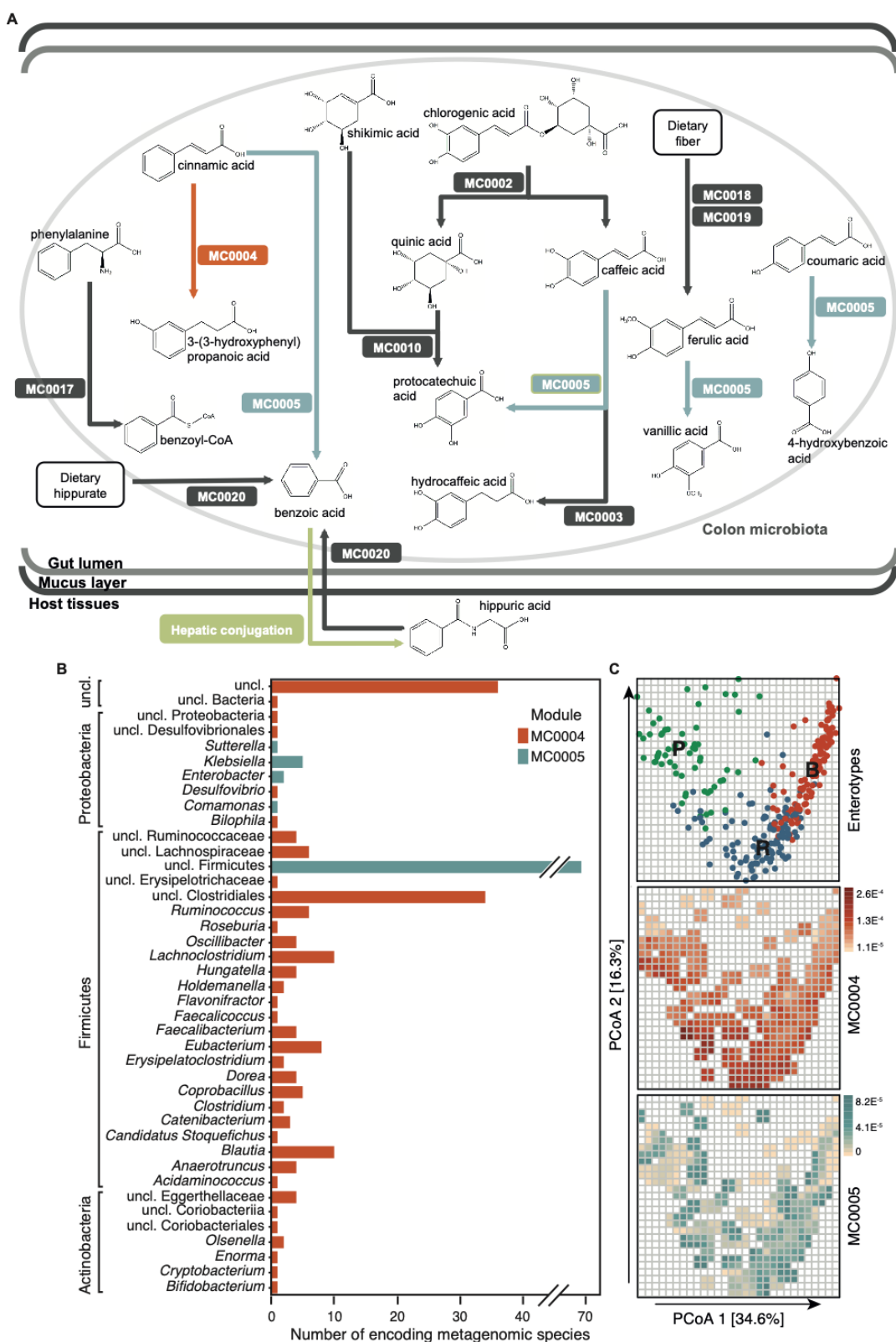
473 The authors declare no competing financial interests.

474 **Figure Legends**



475

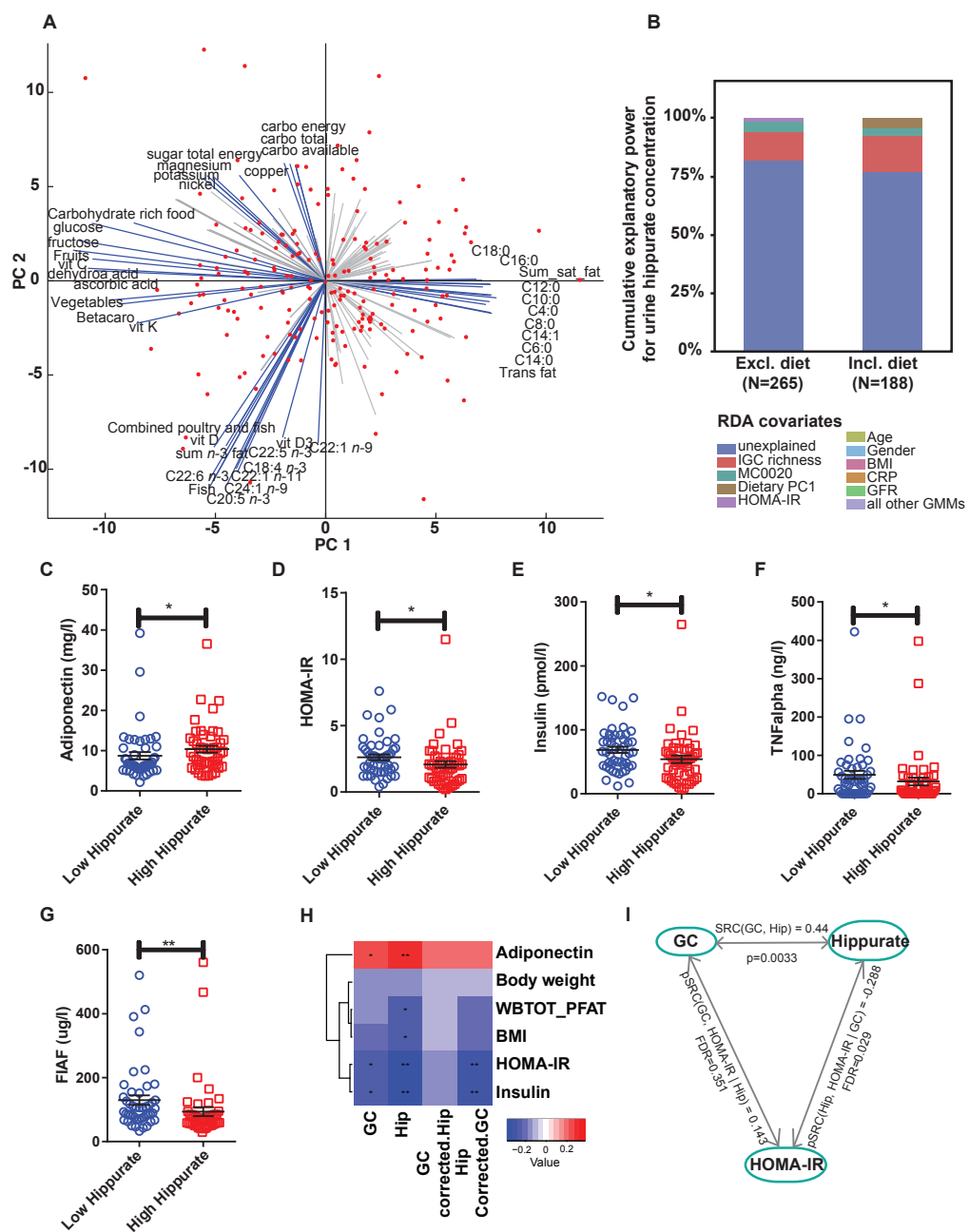
476 **Figure 1. Hippurate is the main metabolite correlated with gene richness and**  
477 **functional redundancy of the microbiome. (A)** Scores plot (predictive component 1)  
478 obtained for an O-PLS-DA model fitted using urinary  $^1\text{H}$  NMR-spectra to predict microbial  
479 gene richness, showing a significant association between gene richness quartiles and  $^1\text{H}$   
480 NMR spectra ( $p=5.84 \times 10^{-21}$  for a significantly non-zero slope using F-test, n=271). **(B)**  
481 Empirical assessment of the significance of O-PLS goodness-of-fit parameter  $Q^2_{Y\hat{h}at}$  by  
482 generating a null distribution with 10,000 random permutations ( $p=9.68 \times 10^{-5}$ ). **(C)** Manhattan  
483 plot highlighting associations between  $^1\text{H}$  NMR variables and gene count displayed in a  
484 pseudo-spectrum layout. A negative value (blue circles) means a negative correlation while  
485 a positive value (red circles) means a positive correlation. Grey circles are clusters with a p-  
486 value  $> 0.01$ . Size of circles represents the covariance of the cluster with the gene count. **(D)**  
487 Association between urinary hippurate intensity and gene count quartiles ( $p=1.99 \times 10^{-9}$  for a  
488 significantly non-zero slope using F-test). **(E)** Association between urinary hippurate intensity  
489 and microbial functional redundancy [26] quartiles ( $p=0.0239$  for a significantly non-zero  
490 slope using F-test, n=271).



491

492 **Figure 2. Detection of microbial phenylpropanoid metabolism-related modules in fecal**  
 493 **metagenomes of healthy volunteers and their associations with urine hippurate**  
 494 **concentrations. (A)** Visualisation of gut-specific metabolic modules (GMMs) encoding  
 495 anaerobic phenylpropanoid metabolism-related pathways detected in more than 20% of

496 individuals; MC0004 (orange; Spearman rho=0.19, q-value=0.005) and MC0005 (blue;  
497 Spearman rho=0.21, q-value=0.005) correlate positively to urine hippurate concentrations  
498 (n=271). All metabolites are connected to benzoate but for clarity the non-significant  
499 reactions were omitted. **(B)** Metagenomic species encoding modules MC0004 and MC0005.  
500 **(C)** [top panel] Fecal microbiomes dissimilarity visualised on the first plane of the genus-level  
501 principal coordinates analysis (PCoA, Bray-Curtis dissimilarity), with individual samples  
502 colored according to enterotypes (R, Ruminococcaceae; B, Bacteroides; P, Prevotella).  
503 [middle and bottom panels] Same genus-level PCoA overlaid with a mesh colored according  
504 to the median abundances of GMMs MC0004 (red) and MC0005 (blue) in samples falling  
505 within each cell of the mesh (n=271). See Supplementary Table S3 for correlation between  
506 hippurate and GMMs.



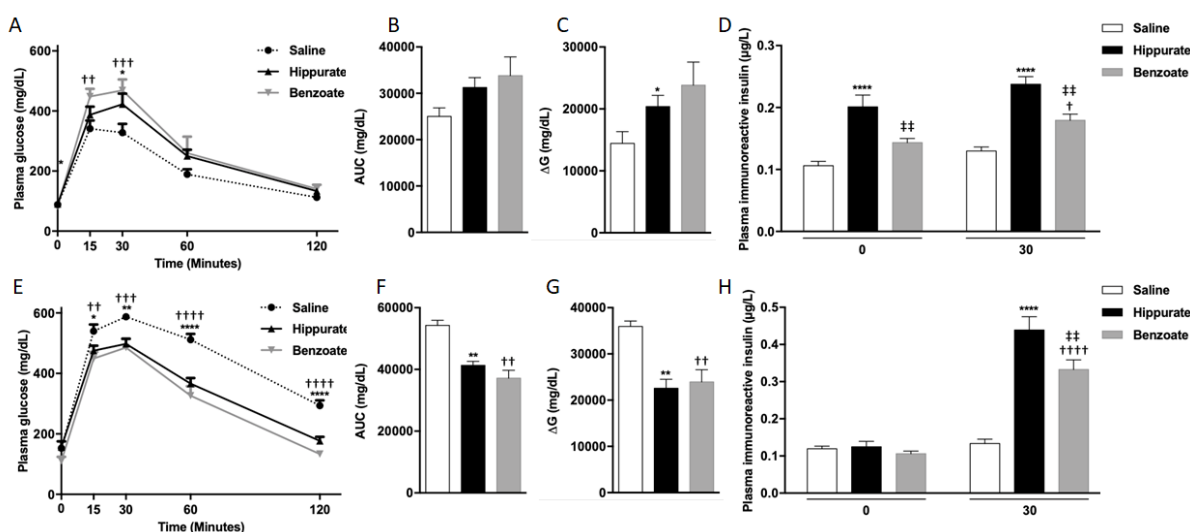
507

508 **Figure 3. Hippurate associates with improved glucose homeostasis only in**  
 509 **participants consuming a diet rich in saturated fats. (A)** Biplot of the principal  
 510 component analysis (PCA) of dietary intakes highlights opposite diets along first two  
 511 principal components (PCs). The main drivers of each principal components are named and  
 512 represented by blue arrows. **(B)** Cumulative contributions of explanatory variables to inter-  
 513 individual variation in hippurate excretion, estimated by redundancy analysis (dbRDA).  
 514 Explanatory variables included microbiota gene count, microbiota phenylpropanoid  
 515 metabolism modules, host dietary principal components and clinical parameters (age,  
 516 gender, BMI, HOMA-IR, CRP, serum glycine levels, and glomerular filtration rate (eGFR)  
 517 estimation with CKD-EPI). **(C-F)** Evaluation of hippurate stratification (high hippurate, n=49

518 vs low hippurate, n=48) on bioclinical variables (q<0.1, Supplementary Table S8) for  
519 individuals on high PC1 (i.e. high meat / high saturated fat diet). For full name description of  
520 physiological data see Supplementary Table S8.

521

522



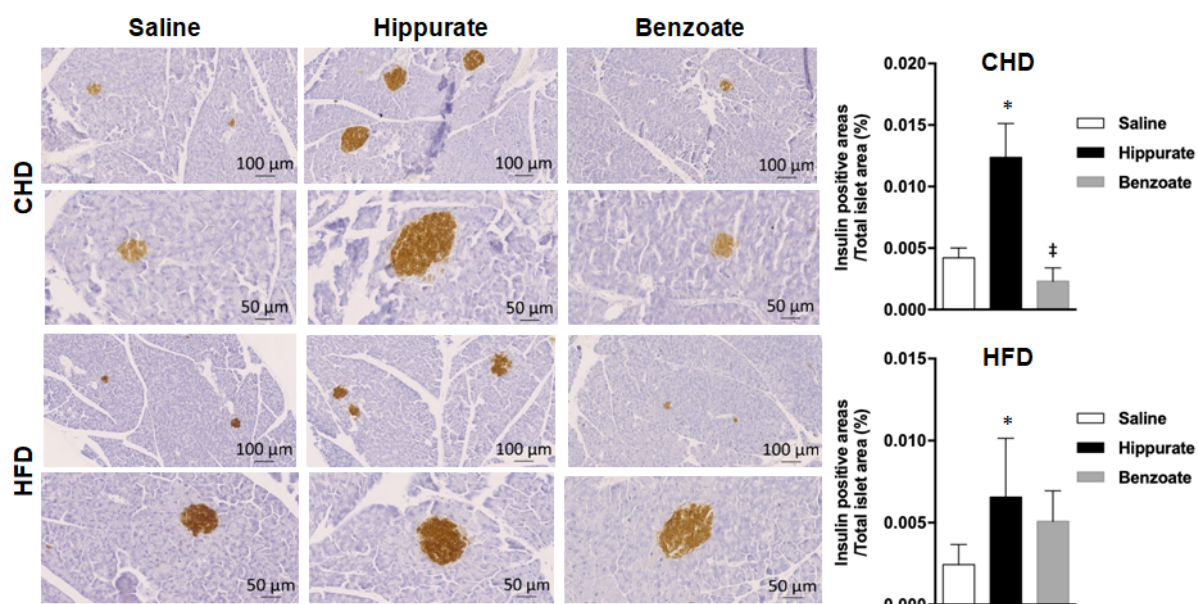
523

524 **Figure 4. Chronic hippurate treatment improves glucose homeostasis in HFD-fed**  
525 **mice.**

526 **(A)** Heatmap summarising Spearman's partial correlation between gene richness,  
527 hippurate, gene richness adjusted for hippurate and hippurate adjusted for gene richness and  
528 bioclinical variables, all correlations adjusted for age and gender. Stars represent significant  
529 pFDR corrected using Benjamini Hochberg procedure \* pFDR<0.1, \*\* pFDR<0.05, \*\*\*  
530 p<0.01. **(B)** Representation of the Spearman's correlations and partial correlations between  
531 gene count and hippurate, hippurate and HOMA-IR adjusted for gene richness and between  
532 gene richness and HOMA-IR adjusted for hippurate. **(C)** Plasma glucose during a glucose  
533 tolerance test (GTT). **(D)** Area under the curve for glucose during the GTT. **(E)** Body weight  
534 of mice during the 6 weeks of hippurate treatment. **(F)** Body mass index at sacrifice **(G)**  
535 Adipose tissue weight normalised to body weight. **(H)** Plasma adiponectin concentration. For  
536 chow diet and chow diet + hippurate, (n=10) and for HFD and HFD + hippurate (n=6). Data  
537 shown are mean±SEM. Statistical analysis was performed using two-way ANOVA with  
538 Tukey's posthoc test. \*\* p<0.01, \*\*\*\* p<0.0001. For panel (D), (F), (G) and (H), groups with  
539 different superscript letters are significantly different (P<0.05), according to Tukey's posthoc  
540 test.

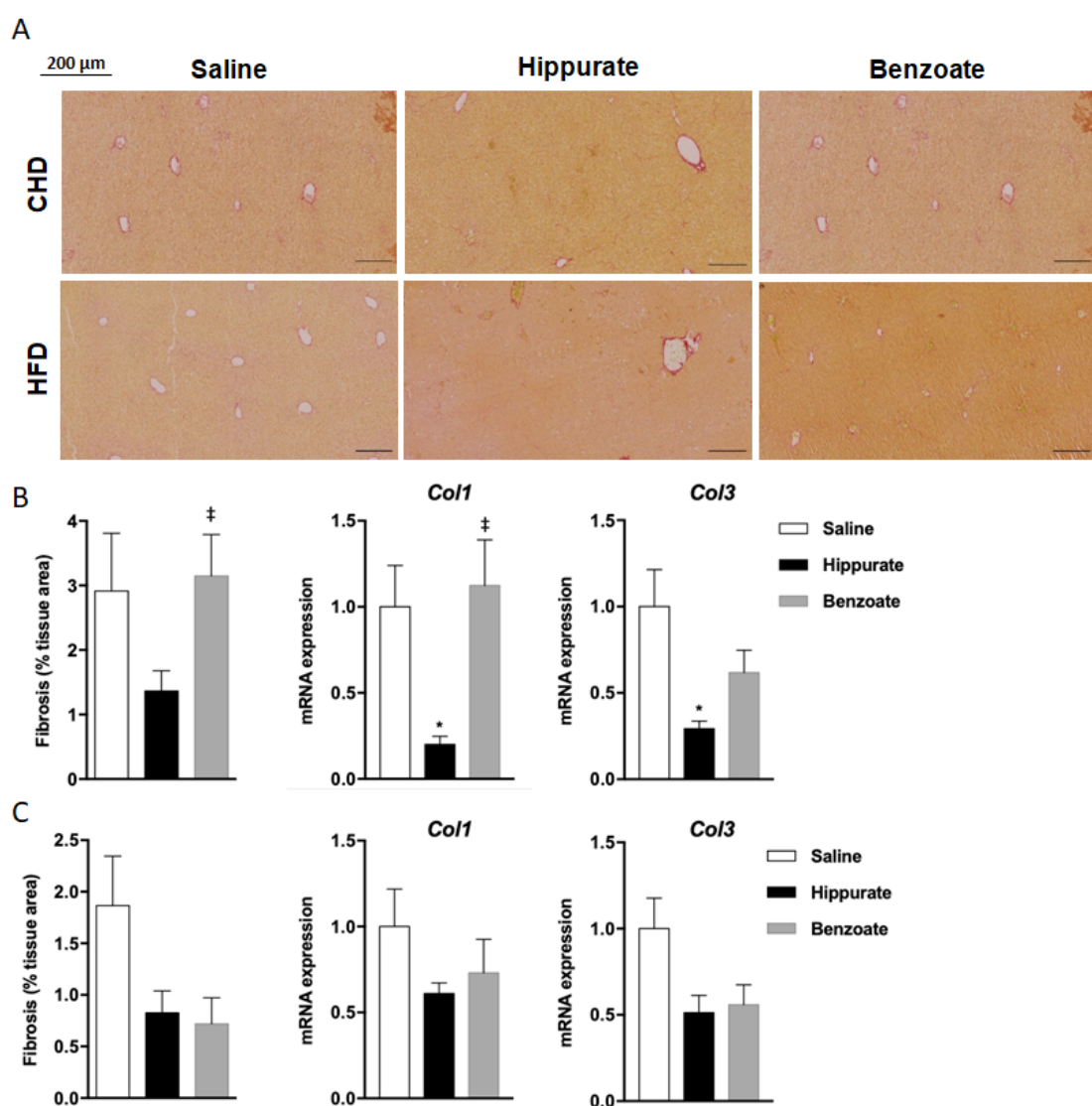
541

542

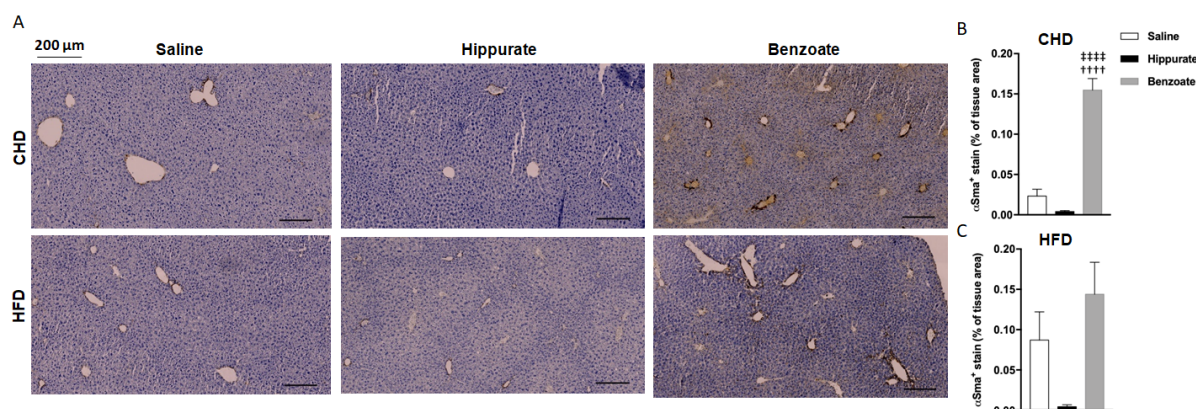


543

544 **Figure 5. Effect of chronic administration of hippurate and benzoate on pancreatic**  
545 **islets in C57BL6/J mice.** The effect of chronic subcutaneous administration of the  
546 metabolites (5.55 mM) for 42 days on islet density was tested in mice fed chow diet (CHD)  
547 or high fat diet (HFD) for 56 days. Control mice were treated with saline. Each biological  
548 replicate represents one slide per animal mounted with at least 3 tissue sections,  
549 representing 3 technical replicates, the mean and variance of which is presented as the  
550 result per biological replicate. Results are expressed as percentage of positive pixels.  
551 ‡P<0.05, significantly different between mice treated with benzoate and hippurate.



552  
553 **Figure 6. Effect of chronic administration of hippurate and benzoate on liver fibrosis**  
554 **(A)**The effect of chronic subcutaneous administration of the metabolites  
555 (5.55 mM) for 42 days on liver collagen was tested in mice fed control chow diet (CHD) or  
556 high fat diet (HFD) for 56 days. Control mice were treated with saline. Red Picosirius  
557 staining of histological sections was used to visualise and quantify fibrosis in mice fed CHD  
558 (**B**) or HFD (**C**). Each biological replicate represents one slide per animal mounted with at  
559 least 3 tissue sections, representing 3 technical replicates, the mean and variance of which  
560 is presented as the result per biological replicate (**B,C**). Liver expression of the genes  
561 encoding collagen 1 (*Col1*) and collagen 3 (*Col3*) was assessed in mice fed CHD (B) or HFD  
562 (**C**) by quantitative RT PCR in 6 mice per group. Data were analyzed using the unpaired  
563 Mann-Whitney test. Results are means  $\pm$  SEM. \* $P<0.05$  significantly different between mice  
564 treated with hippurate and controls.  $\ddagger P<0.05$ , significantly different between mice treated  
565 with benzoate and hippurate.



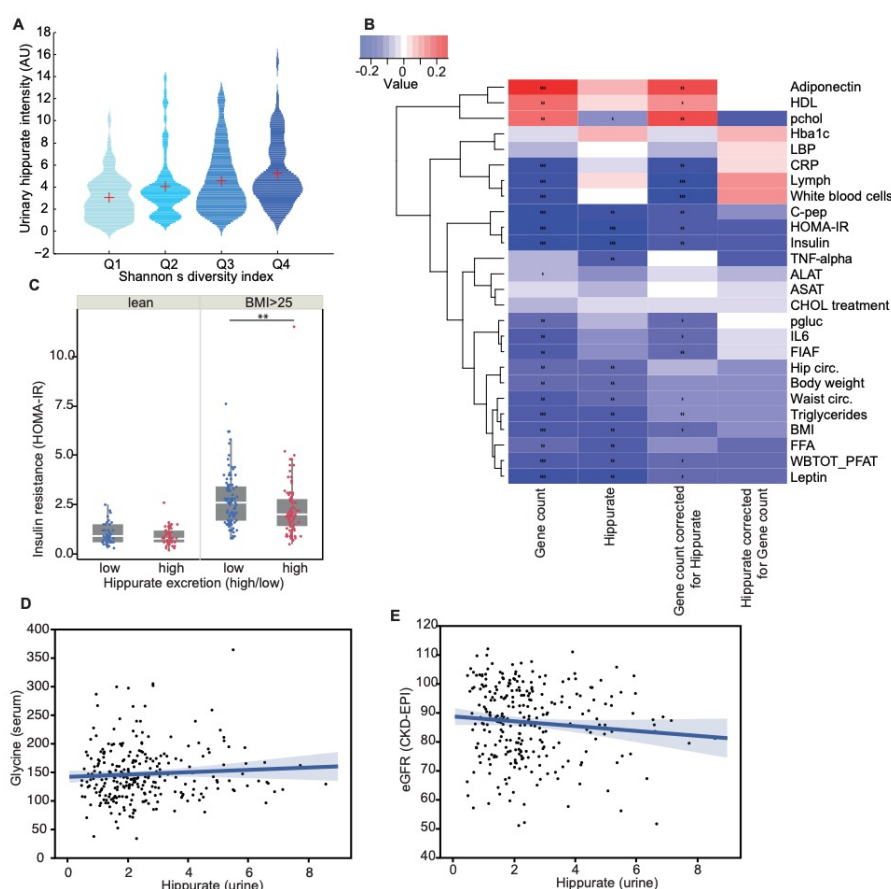
566

567 **Figure 7. Effect of chronic administration of hippurate and benzoate on liver**  
568 **inflammation in C57BL6/J mice.** αSMA staining of liver slides was used to assess  
569 inflammation in mice fed chow diet (CHD) or high fat diet (HFD) for 56 days and chronically  
570 treated with subcutaneous administration of the metabolites (5.55mM) for 42 days (**A**).  
571 Control mice were treated with saline. Each biological replicate represents one slide per  
572 animal mounted with at least 3 tissue sections, representing 3 technical replicates, the mean  
573 and variance of which is presented as the result per biological replicate in mice fed CHD (**B**)  
574 or HFD (**C**). Data were analyzed using the unpaired Mann-Whitney test. Results are means  
575 ± SEM.  
576 †††P<0.0001, significantly different between mice treated with benzoate and saline treated  
577 controls. ‡‡‡P<0.0001, significantly different between mice treated with benzoate and  
578 hippurate.

579

580 **SUPPLEMENTARY SECTION**

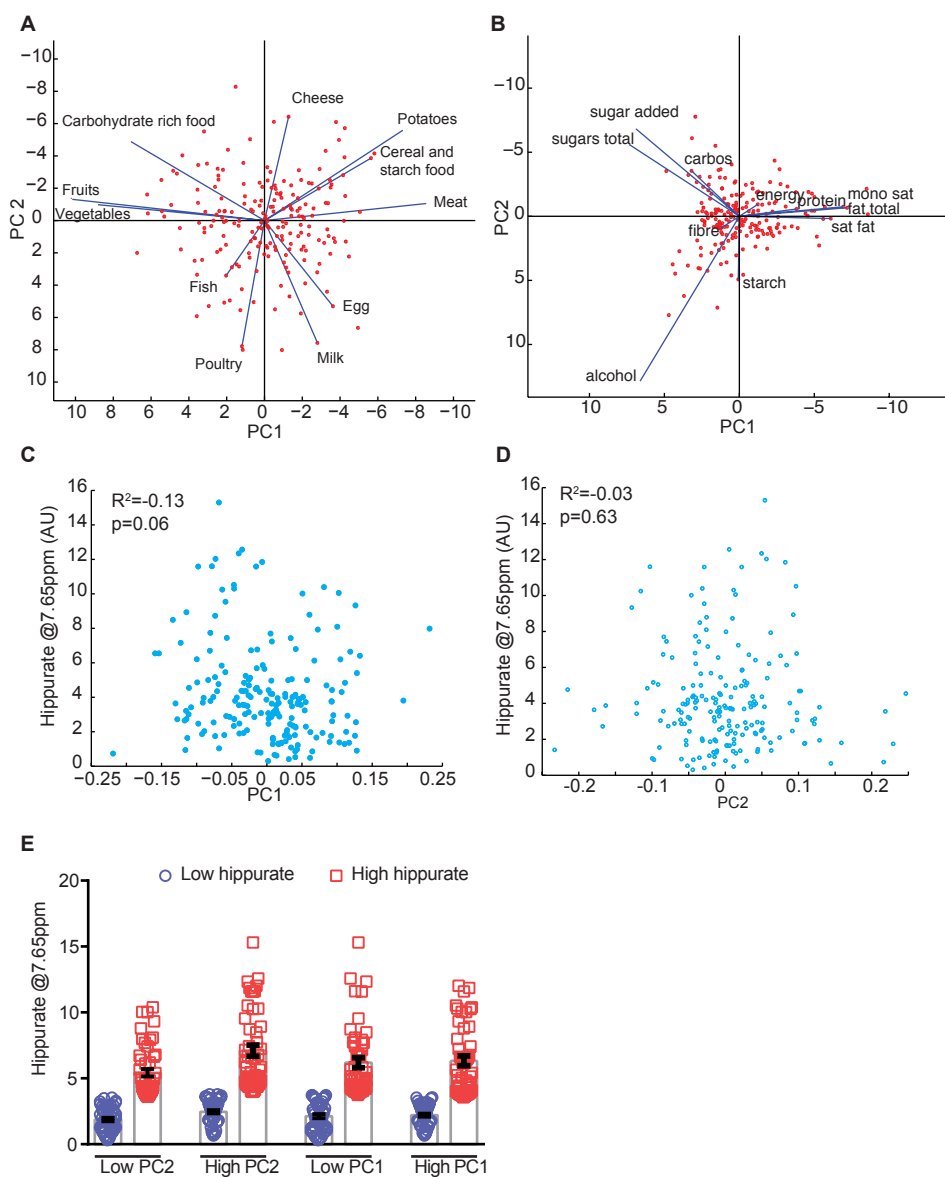
581



582

583 **Supplementary Figure 1. Relationship between gene richness, hippurate and**  
 584 **bioclinical variables**

585 **(A)** Association between urinary hippurate intensity and Shannon's diversity index quartiles  
 586 ( $p=6.04 \times 10^{-8}$  for a significantly non-zero slope using F-test,  $n=271$ ). **(B)** Heatmap  
 587 summarising significant ( $p\text{FDR} < 0.1$ ) Spearman's correlation FDR corrected using Storey's  
 588 procedure[27] between gene count, hippurate and gene count adjusted for hippurate and  
 589 physiological data, all adjusted for age and gender. For full physiological data names and  
 590 units see *Supplementary Table 8*. **(C)** Association between hippurate and insulin resistance  
 591 (HOMA-IR) stratified according to BMI (lean ( $\text{BMI} \leq 25$ ,  $n=87$ ), overweight and obese ( $\text{BMI} > 25$   
 592 , $n=184$ ) and hippurate excretion levels (Mann-Whitney U test,  $p=0.0058$ ). **(D)**  
 593 Representation of the absence of significant correlation between urinary hippurate and  
 594 eGFR. **(E)** Representation of the absence of significant correlation between urinary  
 595 hippurate and circulating glycine.

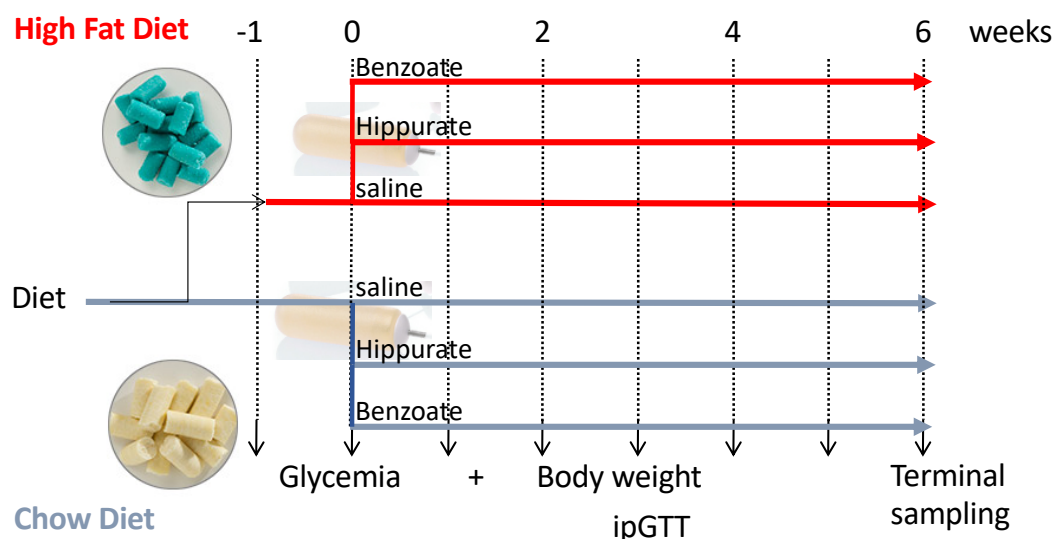


596

597 **Supplementary Figure 2. Urinary hippurate does not correlate with main dietary**

598 **trends summarized and presents a high variability within each subgroup**

599 **(A)** Biplot of the dietary data generated using only food items. **(B)** Biplot of thmicrobial e  
600 dietary data generated using only macronutrients items. **(C)** Representation of the absence  
601 of correlation between hippurate concentration and principal component 1. **(D)**  
602 Representation of the absence of correlation between hippurate concentration and principal  
603 component 2. **(E)** Distribution of hippurate urinary concentration within each  
604 individualsubgroup stratified in high and low hippurate using median.



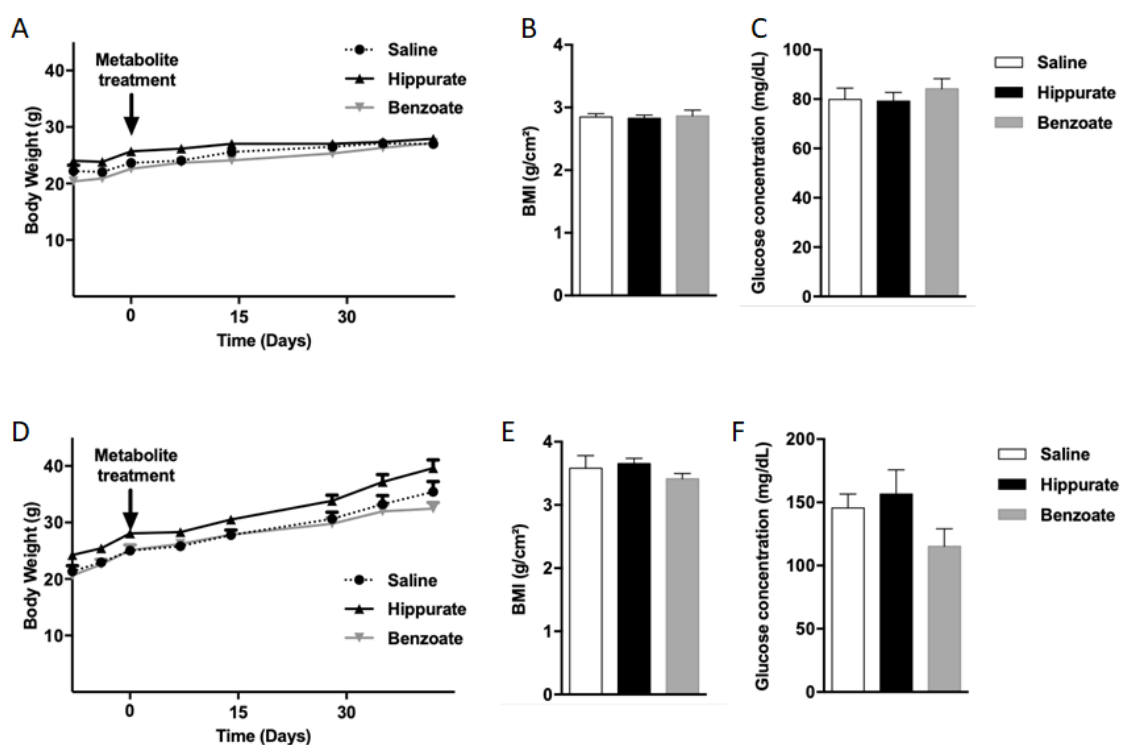
605

606 **Supplementary Figure 3. Experimental design for chronic six-week administration of**  
607 **benzoate and hippurate**

608 Experiment design showing groups and durations of each step for the chronic treatments  
609 with benzoate and hippurate in mice.

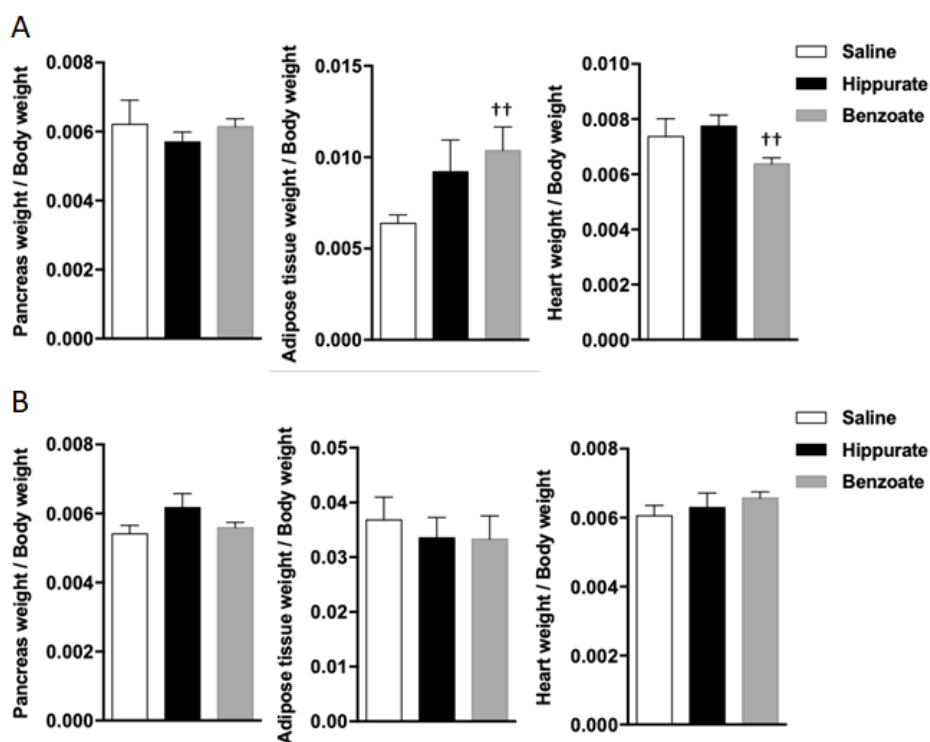
610

611



612

613 **Supplementary Figure 4. Effects of chronic administration of hippurate and benzoate**  
614 **on body growth and fasting glycemia.** C57BL6/J mice fed control chow diet (**A-C**) or high  
615 fat diet (**D-F**). The effects of chronic subcutaneous administration of the metabolites (5.55  
616 mM) in mice were tested on body weight (**A,D**), body mass index (BMI) (**B,E**), fasting  
617 glycemia (**C,F**). Control mice were treated with saline. BMI was calculated as body weight  
618 divided by the squared of anal-nasal length. Results are means  $\pm$  SEM.



619

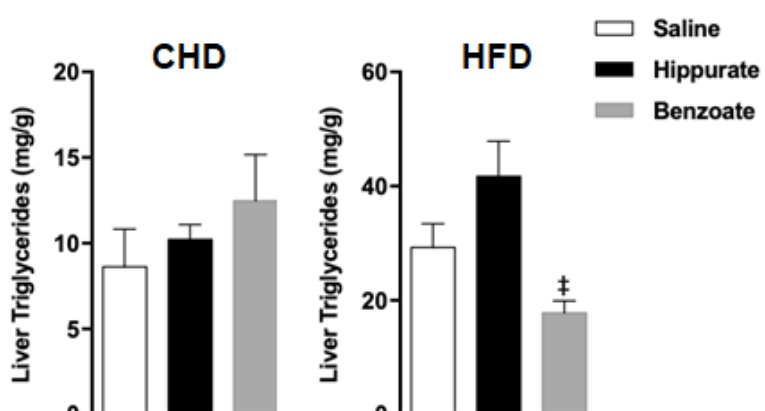
620 **Supplementary Figure 5.** Organ weight in C57BL6/J mice treated chronically with hippurate  
621 or benzoate for 42 days. Control mice were treated with saline. Mice were fed chow diet  
622 (CHD) or high fat diet (HFD) for 56 days. Data are expressed as the ratio between organ  
623 weight and body weight. Data were analyzed using the unpaired Mann-Whitney test. Results  
624 are means  $\pm$  SEM.

625 \*\*P<0.01, significantly different between mice treated with hippurate and controls. †P< 0.05,

626 ††P<0.01, significantly different between mice treated with benzoate and saline treated  
627 controls.

628

629



630

631 **Supplementary Figure 6. Effect of chronic administration of hippurate and benzoate**  
632 **on liver triglycerides content in C57BL6/J mice.** The effect of chronic subcutaneous  
633 administration of the metabolites (5.55mM) for 42 days on liver triglycerides was tested in  
634 mice fed control chow diet (CHD) or high fat diet (HFD) for 56 days. Assay was carried out in  
635 6 mice per group. Data were analyzed using the unpaired Mann-Whitney test.

636 Results are means  $\pm$  SEM

637  $\ddagger P < 0.05$ , significantly different between mice treated with benzoate and hippurate.

638

639

640 **Supplementary Table S1**

641 Association between microbiota functional potential mapped to KEGG Orthologs (KOs)  
642 database and urine hippurate levels.

643

644 **Supplementary Table S2**

645 Association between microbiota functional potential mapped to the eggNOG database and  
646 urine hippurate levels.

647

648 **Supplementary Table S3**

649 Association between microbiota functional potential mapped to gut-specific metabolic  
650 modules (GMMs) describing phenylpropanoid metabolism and urine hippurate levels.

651

652 **Supplementary Table S4**

653 Association between abundance of gut-specific metabolic modules (GMMs) describing  
654 phenylpropanoid metabolism and gene richness.

655

656 **Supplementary Table S5**

657 Phenylpropanoid metabolism potential in metagenomic species, assessed by mapping to  
658 GMMs significantly associated to urine hippurate levels.

659

660 **Supplementary Table S6**

661 Association between the microbiota composition profiled as metagenomic OTUs (mOTUs)  
662 and urine hippurate levels.

663

664 **Supplementary Table S7**

665 pFDR from Spearman's rank-based correlations between GMMs describing  
666 phenylpropanoid metabolism and gene richnessbioclinical variables using Storey's FDR  
667 correction.

668

669 **Supplementary Table 8**

670 pFDR from Mann-Whitney U test for hippurate stratification in each bioclinical variable  
671 between using Storey's FDR correction.

672

673

674 **REFERENCES**

675 1 Lynch SV, Pedersen O. The Human Intestinal Microbiome in Health and Disease. *N  
676 Engl J Med* 2016; **375**:2369–79. doi:10.1056/NEJMra1600266

677 2 Li J, Jia H, Cai X, *et al.* An integrated catalog of reference genes in the human gut  
678 microbiome. *Nat Biotechnol* 2014; **32**:834–41. doi:10.1038/nbt.2942

679 3 Qin J, Li R, Raes J, *et al.* A human gut microbial gene catalogue established by  
680 metagenomic sequencing. *Nature* 2010; **464**:59–65. doi:10.1038/nature08821

681 4 Le Chatelier E, Nielsen T, Qin J, *et al.* Richness of human gut microbiome correlates  
682 with metabolic markers. *Nature* 2013; **500**:541–6. doi:10.1038/nature12506

683 5 Cotillard A, Kennedy SP, Kong LC, *et al.* Dietary intervention impact on gut microbial  
684 gene richness. *Nature* 2013; **500**:585–8. doi:10.1038/nature12480

685 6 Nicholson JK, Holmes E, Wilson ID. Gut microorganisms, mammalian metabolism and  
686 personalized health care. *Nat Rev Microbiol* 2005; **3**:431–8. doi:10.1038/nrmicro1152

687 7 Dumas M-E. The microbial-mammalian metabolic axis: beyond simple metabolism. *Cell  
688 Metab* 2011; **13**:489–90. doi:10.1016/j.cmet.2011.04.005

689 8 Nicholson JK, Holmes E, Kinross J, *et al.* Host-gut microbiota metabolic interactions.  
690 *Science* 2012; **336**:1262–7. doi:10.1126/science.1223813

691 9 Neves AL, Chilloux J, Sarafian MH, *et al.* The microbiome and its pharmacological  
692 targets: therapeutic avenues in cardiometabolic diseases. *Curr Opin Pharmacol*  
693 2015; **25**:36–44. doi:10.1016/j.coph.2015.09.013

694 10 Dumas M-E, Barton RH, Toye A, *et al.* Metabolic profiling reveals a contribution of gut  
695 microbiota to fatty liver phenotype in insulin-resistant mice. *Proc Natl Acad Sci USA*  
696 2006; **103**:12511–6. doi:10.1073/pnas.0601056103

697 11 Holmes E, Loo RL, Stamler J, *et al.* Human metabolic phenotype diversity and its  
698 association with diet and blood pressure. *Nature* 2008; **453**:396–400.  
699 doi:10.1038/nature06882

700 12 Elliott P, Posma JM, Chan Q, *et al.* Urinary metabolic signatures of human adiposity.  
701 *Sci Transl Med* 2015; **7**:285ra62. doi:10.1126/scitranslmed.aaa5680

702 13 Pallister T, Jackson MA, Martin TC, *et al.* Untangling the relationship between diet and  
703 visceral fat mass through blood metabolomics and gut microbiome profiling. *Int J Obes  
(Lond)* 2017; **41**:1106–13. doi:10.1038/ijo.2017.70

705 14 Hoyles L, Fernández-Real JM, Federici M, *et al.* Molecular phenomics and  
706 metagenomics of hepatic steatosis in non-diabetic obese women. *Nat Med*  
707 2018; **24**:1070–80. doi:10.1038/s41591-018-0061-3

708 15 Lees HJ, Swann JR, Wilson ID, *et al.* Hippurate: The Natural History of a Mammalian-  
709 Microbial Cometabolite. *J Proteome Res* 2013; **12**:1527–46. doi:10.1021/pr300900b

710 16 Dumas M-E, Wilder SP, Bihoreau M-T, *et al.* Direct quantitative trait locus mapping of  
711 mammalian metabolic phenotypes in diabetic and normoglycemic rat models. *Nat Genet* 2007;39:666–72. doi:10.1038/ng2026

713 17 Pallister T, Jackson MA, Martin TC, *et al.* Hippurate as a metabolomic marker of gut  
714 microbiome diversity: Modulation by diet and relationship to metabolic syndrome.  
715 *Scientific Reports* 2017;7:13670. doi:10.1038/s41598-017-13722-4

716 18 Pedersen HK, Gudmundsdottir V, Nielsen HB, *et al.* Human gut microbes impact host  
717 serum metabolome and insulin sensitivity. *Nature* 2016;535:376–81.  
718 doi:10.1038/nature18646

719 19 Forslund K, Hildebrand F, Nielsen T, *et al.* Disentangling type 2 diabetes and metformin  
720 treatment signatures in the human gut microbiota. *Nature* 2015;528:262–6.  
721 doi:10.1038/nature15766

722 20 Jørgensen T, Borch-Johnsen K, Thomsen TF, *et al.* A randomized non-pharmacological  
723 intervention study for prevention of ischaemic heart disease: baseline results Inter99.  
724 *Eur J Cardiovasc Prev Rehabil* 2003;10:377–86.  
725 doi:10.1097/01.hjr.0000096541.30533.82

726 21 Levey AS, Stevens LA, Schmid CH, *et al.* A new equation to estimate glomerular  
727 filtration rate. *Ann Intern Med* 2009;150:604–12.

728 22 Toft U, Kristoffersen L, Ladelund S, *et al.* Relative validity of a food frequency  
729 questionnaire used in the Inter99 study. *Eur J Clin Nutr* 2008;62:1038–46.  
730 doi:10.1038/sj.ejcn.1602815

731 23 Dona AC, Jiménez B, Schäfer H, *et al.* Precision high-throughput proton NMR  
732 spectroscopy of human urine, serum, and plasma for large-scale metabolic  
733 phenotyping. *Anal Chem* 2014;86:9887–94. doi:10.1021/ac5025039

734 24 Blaise BJ, Shintu L, Elena B, *et al.* Statistical recoupling prior to significance testing in  
735 nuclear magnetic resonance based metabonomics. *Anal Chem* 2009;81:6242–51.  
736 doi:10.1021/ac9007754

737 25 Dona AC, Kyriakides M, Scott F, *et al.* A guide to the identification of metabolites in  
738 NMR-based metabonomics/metabolomics experiments. *Comput Struct Biotechnol J*  
739 2016;14:135–53. doi:10.1016/j.csbj.2016.02.005

740 26 Vieira-Silva S, Falony G, Darzi Y, *et al.* Species-function relationships shape ecological  
741 properties of the human gut microbiome. *Nat Microbiol* 2016;1:16088.  
742 doi:10.1038/nmicrobiol.2016.88

743 27 Storey JD, Tibshirani R. Statistical significance for genomewide studies. *Proc Natl Acad  
744 Sci USA* 2003;100:9440–5. doi:10.1073/pnas.1530509100

745 28 Dixon P. VEGAN, a package of R functions for community ecology. *Journal of  
746 Vegetation Science* 2003;14:927–30. doi:10.1111/j.1654-1103.2003.tb02228.x

747 29 Cloarec O, Dumas ME, Trygg J, *et al.* Evaluation of the orthogonal projection on latent  
748 structure model limitations caused by chemical shift variability and improved  
749 visualization of biomarker changes in <sup>1</sup>H NMR spectroscopic metabonomic studies.  
750 *Anal Chem* 2005;77:517–26. doi:10.1021/ac048803i

751 30 Blaise BJ, Giacomotto J, Elena B, *et al.* Metabotyping of *Caenorhabditis elegans*  
752 reveals latent phenotypes. *Proc Natl Acad Sci USA* 2007;104:19808–12.  
753 doi:10.1073/pnas.0707393104

754 31 Brial F, Le Lay A, Hedjazi L, *et al.* Systems Genetics of Hepatic Metabolome Reveals  
755 Octopamine as a Target for Non-Alcoholic Fatty Liver Disease Treatment. *Scientific*  
756 *Reports* 2019;9:3656. doi:10.1038/s41598-019-40153-0

757 32 Phipps AN, Stewart J, WRIGHT B, *et al.* Effect of diet on the urinary excretion of  
758 hippuric acid and other dietary-derived aromatics in rat. A complex interaction between  
759 diet, gut microflora and substrate specificity. *Xenobiotica* 1998;28:527–37.  
760 doi:10.1080/004982598239443

761 33 Backhed F, Ding H, Wang T, *et al.* The gut microbiota as an environmental factor that  
762 regulates fat storage. *Proc Natl Acad Sci USA* 2004;101:15718–23.  
763 doi:10.1073/pnas.0407076101

764 34 Bridle KR, Crawford DHG, Ramm GA. Identification and characterization of the hepatic  
765 stellate cell transferrin receptor. *Am J Pathol* 2003;162:1661–7. doi:10.1016/S0002-  
766 9440(10)64300-3

767 35 Shi J, Zhao J, Zhang X, *et al.* Activated hepatic stellate cells impair NK cell anti-fibrosis  
768 capacity through a TGF- $\beta$ -dependent emperipolesis in HBV cirrhotic patients. *Scientific*  
769 *Reports* 2017;7:44544. doi:10.1038/srep44544

770 36 Aron-Wisnewsky J, Prifti E, Belda E, *et al.* Major microbiota dysbiosis in severe obesity:  
771 fate after bariatric surgery. *Gut* 2019;68:70–82. doi:10.1136/gutjnl-2018-316103

772 37 Akira K, Masu S, Imachi M, *et al.*  $^1\text{H}$  NMR-based metabonomic analysis of urine from  
773 young spontaneously hypertensive rats. *J Pharm Biomed Anal* 2008;46:550–6.  
774 doi:10.1016/j.jpba.2007.11.017

775 38 Zhao L-C, Zhang X-D, Liao S-X, *et al.* A metabonomic comparison of urinary changes  
776 in Zucker and GK rats. *J Biomed Biotechnol* 2010;2010:431894–6.  
777 doi:10.1155/2010/431894

778 39 Pontoizeau C, Fearnside JF, Nayratil V, *et al.* Broad-Ranging Natural Metabotype  
779 Variation Drives Physiological Plasticity in Healthy Control Inbred Rat Strains. *J*  
780 *Proteome Res* 2011;10:1675–89. doi:10.1021/pr101000z

781 40 Bitner BF, Ray JD, Kener KB, *et al.* Common gut microbial metabolites of dietary  
782 flavonoids exert potent protective activities in  $\beta$ -cells and skeletal muscle cells. *J Nutr*  
783 *Biochem* 2018;62:95–107. doi:10.1016/j.jnutbio.2018.09.004

784 41 Dumas M-E, Rothwell AR, Hoyles L, *et al.* Microbial-Host Co-metabolites Are  
785 Prodromal Markers Predicting Phenotypic Heterogeneity in Behavior, Obesity, and  
786 Impaired Glucose Tolerance. *Cell Rep* 2017;20:136–48.  
787 doi:10.1016/j.celrep.2017.06.039

788 42 Thaiss CA, Itav S, Rothschild D, *et al.* Persistent microbiome alterations modulate the  
789 rate of post-dieting weight regain. *Nature* 2016;540:540–51. doi:10.1038/nature20796

790 43 Patterson AD, Turnbaugh PJ. Microbial determinants of biochemical individuality and  
791 their impact on toxicology and pharmacology. *Cell Metab* 2014;**20**:761–8.  
792 doi:10.1016/j.cmet.2014.07.002

793 44 Shoaei S, Ghaffari P, Kovatcheva-Datchary P, *et al.* Quantifying Diet-Induced Metabolic  
794 Changes of the Human Gut Microbiome. *Cell Metab* 2015;**22**:320–31.  
795 doi:10.1016/j.cmet.2015.07.001

796 45 Zeevi D, Korem T, Zmora N, *et al.* Personalized Nutrition by Prediction of Glycemic  
797 Responses. *Cell* 2015;**163**:1079–94. doi:10.1016/j.cell.2015.11.001

## Supplementary List: Module definitions

### **MC0001 phenylalanine degradation (cinnamate production)**

cpd [phenylalanine] [cinnamate, NH3]

K10775

ref MetaCyc Pathway: trans-cinnamoyl-CoA biosynthesis

### **MC0002 chlorogenate degradation**

cpd [chlorogenate] [caffeate, quinate]

K06889 K09252

ref MetaCyc Pathway: chlorogenic acid degradation <sup>1</sup>

### **MC0003 caffeate respiration**

cpd [caffeate] [hydrocaffeate]

bactNOG04579

ref <sup>2</sup>

### **MC0004 cinnamate conversion**

cpd [cinnamate] [3-(3-hydroxyphenyl)propanoate]

K10797

ref KEGG Pathway: phenylalanine degradation

### **MC0005 coumarate degradation**

cpd [coumarate] [hydroxybenzoate]

cpd [ferulate] [vanillate]

cpd [caffeate] [protocatechuate]

cpd [cinnamate] [benzoate]

K01904 bactNOG05057

K01692 K01715 K01782 K01825 K13767 K15016 bactNOG19280

K00141

ref MetaCyc Pathway: 4-coumarate degradation (anaerobic) 3

**MC0006 (hydroxy)benzoate degradation**

cpd [(hydroxy)benzoate] [3-hydroxypimeloyl-CoA]

K04105,K04107,K04108,K04109 K04110 bactNOG00950

K04112,K04113,K04114,K04115 K19515,K19516

K07537

K07538

K07539

ref MetaCyc Pathway: 4-coumarate degradation (anaerobic) MetaCyc Pathway: benzoyl-CoA  
degradation II (anaerobic) Kegg module: M00541

**MC0007 ferulate degradation**

cpd [ferulate] [vanillin]

K12508

K18383

ref MetaCyc Pathway: ferulate degradation

**MC0008 vanillate conversion**

cpd [vanillin, (O2)] [protocatechuate]

bactNOG00059

K03862,K03863 K15066

ref MetaCyc Pathway: superpathway of vanillin and vanillate degradation Kegg Pathway:  
aminobenzoate degradation

**MC0009 cinnamate degradation**

cpd [cinnamate] [benzoyl-CoA]

bactNOG08521

actNOG07134

COG0277

bactNOG05297

ref MetaCyc Pathway: trans-cinnamoyl-CoA biosynthesis MetaCyc Pathway: benzoyl-CoA biosynthesis

**MC0010 quinate degradation**

cpd [quinate] [protocatechuate]

cpd [shikimate] [protocatechuate]

K05358 COG0169

K03785 K03786 K13832

K09483 K15652

ref MetaCyc Pathway: quinate degradation I MetaCyc Pathway: quinate degradation II  
4

**MC0011 4-hydroxybenzoate conversion**

cpd [4-hydroxybenzoate, O2] [protocatechuate]

K00481

ref Kegg Pathway: benzoate degradation 4 5

**MC0012 catechin degradation**

cpd [catechin] [protocatechuate, phloroglucinol carboxylic acid]

bactNOG14887

ref 6

**MC0013 3-hydroxybenzoate conversion**

cpd [3-hydroxybenzoate, O2] [protocatechuate]

K19065

ref Kegg Pathway: benzoate degradation

**MC0014 benzoate conversion**

cpd [benzoate, O2] [4-hydroxybenzoate]

K07824

ref Kegg Pathway: benzoate degradation

**MC0015            benzoate degradation (aerobic)**

cpd [benzoate, O2] [catechol, CO2]

K05549,K05550,K05784

K05783

ref Kegg module: M00551 MetaCyc Pathway: benzoate degradation I (aerobic)

**MC0016            benzoate degradation (anaerobic)**

cpd [benzoyl-CoA] [3-hydroxypimeloyl-CoA]

K04112,K04113,K04114,K04115 K19515,K19516

K19066

K07534

K07535

K07536

K04118

ref MetaCyc Pathway: benzoyl-CoA degradation III (anaerobic)            Kegg module: M00540

**MC0017            phenylalanine degradation**

cpd [phenylalanine, 2-oxoglutarate] [CO2, glutamate, benzoyl-CoA]

K00832 K00812 K00813 K11358 K00817

K04103

K00146 K00129

K01912

K18361

K18355,K18356,K18357,K18358,K18359

ref MetaCyc Pathway: phenylacetate degradation II (anaerobic) MetaCyc Pathway: L-phenylalanine degradation II (anaerobic)

**MC0018 cellulose and hemicellulose degradation (cellulolosome)**

cpd [cellulose, hemicellulose] [ferulate, polysaccharide, oligosaccharide]

K01181 K13465

K09252

bactNOG05428

ref MetaCyc Pathway: cellulose and hemicellulose degradation (cellulolosome)

**MC0019 feruloyl esterase (cellulolosome)**

cpd [cellulose, hemicellulose] [ferulate]

K09252

ref MetaCyc Pathway: cellulose and hemicellulose degradation (cellulolosome) MC0018

**MC0020 hippurate hydrolase**

cpd [hippurate] [glycine, benzoate]

K01451

ref 7

**References**

1. Couteau, D., McCartney, A. L., Gibson, G. R., Williamson, G. & Faulds, C. B. Isolation and characterization of human colonic bacteria able to hydrolyse chlorogenic acid. *J. Appl. Microbiol.* **90**, 873–881 (2001).
2. Hess, V., González, J. M., Parthasarathy, A., Buckel, W. & Müller, V. Caffeate respiration in the acetogenic bacterium *Acetobacterium woodii*: a coenzyme A loop saves energy for caffeate activation. *Appl. Environ. Microbiol.* **79**, 1942–1947 (2013).
3. Hirakawa, H., Schaefer, A. L., Greenberg, E. P. & Harwood, C. S. Anaerobic p-coumarate degradation by *Rhodopseudomonas palustris* and identification of CouR, a MarR repressor protein that binds p-coumaroyl coenzyme A. *J. Bacteriol.* **194**, 1960–1967 (2012).
4. Brzostowicz, P. C., Reams, A. B., Clark, T. J. & Neidle, E. L. Transcriptional cross-regulation of the catechol and protocatechuate branches of the beta-ketoadipate pathway contributes to carbon source-dependent expression of the *Acinetobacter* sp. strain ADP1 *pobA* gene. *Appl. Environ.*

*Microbiol.* **69**, 1598–1606 (2003).

- 5. Gonthier, M.-P. *et al.* Metabolism of dietary procyanidins in rats. *Free Radic. Biol. Med.* **35**, 837–844 (2003).
- 6. Arunachalam, M., Mohan, N. & Mahadevan, A. Cloning of *Acinetobacter calcoaceticus* chromosomal region involved in catechin degradation. *Microbiol. Res.* **158**, 37–46 (2003).
- 7. Caner, V., Cokal, Y., Cetin, C., Sen, A. & Karagenc, N. The detection of *hipO* gene by real-time PCR in thermophilic *Campylobacter* spp. with very weak and negative reaction of hippurate hydrolysis. *Antonie Van Leeuwenhoek* **94**, 527–532 (2008).